

# Formation, Preservation, and Cleavage of the Disulfide Bond by Vanadium

Dongren Wang, Axel Behrens, Mahin Farahbakhsh, Jessica Gätjens, and Dieter Rehder\*<sup>[a]</sup>

**Abstract:** Reaction of the disulfide {HpicanS}<sub>2</sub> (HpicanS is the carboxamide based on picolinate (pic) and *o*-mercaptoaniline (anS); the {} brackets are used to denote disulfides) with [VOCl<sub>2</sub>(thf)<sub>2</sub>] leads to reductive scission of the disulfide bond and formation of the mixed-valence (V<sup>IV</sup>/V<sup>V</sup>) complex anion [(OV-picanS)<sub>2</sub>μ-O]<sup>-</sup> (**1**), with the dianionic ligand coordinating through the pyridine-*N* atom, the deprotonated amide-*N* atom, and thiophenolate-*S* atom. Reductive cleavage of the S–S bond is also observed as [VCl<sub>2</sub>(tmeda)<sub>2</sub>] (tmeda = tetramethylethylenediamine) is treated with the disulfides {HsalanS}<sub>2</sub> or {HvananS}<sub>2</sub> (HsalanS and HvananS are the Schiff bases formed between *o*-mercaptoaniline and salicylaldehyde (Hsal) or vanillin (Hvan), respectively), yielding the V<sup>III</sup> complexes [VCl(tmeda)-

(salanS)] (**2a**), or [VCl(tmeda)-(vananS)] (**2b**). The disulfide bond remains intact in the aerial reaction between {HsalanS}<sub>2</sub> and [VCl<sub>3</sub>(thf)<sub>3</sub>] to yield the V<sup>V</sup> complex [VOCl{salanS}<sub>2</sub>] (**3**), where (salanS)<sup>2-</sup> coordinates through the two phenolate and one of the imine functions. The S–S bond is also preserved as [VO(van)<sub>2</sub>] or [VO(nap)<sub>2</sub>] (Hnap = 2-hydroxynaphthalene-1-carbaldehyde) is treated with bis-(2-aminophenyl)disulfide, {anS}<sub>2</sub>, a reaction which is accompanied by condensation of the aldehyde and the diamine, and complexation of the resulting bis-(Schiff bases) {HvananS}<sub>2</sub> or {HnapanS}<sub>2</sub>

to form the complexes [VO{vananS}<sub>2</sub>] (**4a**) or [VO{napanS}<sub>2</sub>] (**4b**). In **4a** and **4b**, the phenolate and imine functions, and presumably also one of the disulfide-S atoms, coordinate to V<sup>V</sup>. 2-Mercaptophenyl-2'-pyridinecarboxamide (H<sub>2</sub>picanS) retains its identity in the presence of V<sup>III</sup>; reaction between [VCl<sub>3</sub>(thf)<sub>3</sub>] and H<sub>2</sub>picanS yields [V{picanS}<sub>2</sub>]<sup>-</sup> (**5**). The dithiophenolate 2,6-bis(mercaptophenylthio)dimethylpyridine (**6a**) is oxidized, mediated by VO<sup>2+</sup>, to the bis(disulfide) octathiadiazacyclo-hexaeicosane **6b**. The relevance of these reactions for the speciation of vanadium under physiological conditions is addressed. [HNEt<sub>3</sub>]-1·0.5NEt<sub>3</sub>, **3**·3CH<sub>2</sub>Cl<sub>2</sub>, {HsalanS}<sub>2</sub>, [HNEt<sub>3</sub>]-**5**, and **6b**·4THF have been characterized by X-ray diffraction analysis.

**Keywords:** amides · biomimetic synthesis · disulfides · S ligands · vanadium

## Introduction

There is continuing interest in studies towards the coordination of thiofunctional ligands to vanadium<sup>[1]</sup> in the context of enzymes containing vanadium in the active center, since these investigations can model the specific bonding situation and thus reactivity of the vanadium cofactor. Examples are vanadium-nitrogenase from *Azotobacter*, where vanadium—in analogy to its molybdenum counter-part—is coordinated to, inter alia, three sulfides,<sup>[2]</sup> and vanadium-containing nitrate reductase from *A. vinelandii*,<sup>[3]</sup> which—again in analogy to the more common Mo analogue<sup>[4]</sup>—probably contains dithiolenate (as a constituent of a pyranopterin moiety) attached to the oxo-metal center. Furthermore, the sulfide peroxidase activity of vanadate-dependent haloperoxidases<sup>[5]</sup> suggests

the formation of an intermediate where the organic sulfide is in contact with the active center, since formation of sulfoxide from prochiral sulfides occurs enantioselectively. Likewise, sulfide- and disulfide–vanadium intermediates supposedly form in the enantioselective oxo transfer to sulfides<sup>[6, 7]</sup> and disulfides<sup>[8]</sup> with oxovanadium Schiff base<sup>[6, 8]</sup> and oxovanadium–ethanolamine systems.<sup>[7]</sup>

An additional, and an equally important aspect of the vanadium–sulfur interaction is the redox and nonredox inhibition by vanadate of phosphatases containing cysteine in their active centers.<sup>[9, 10]</sup> Vanadate may coordinate to the active center cysteine, forming a coordination environment very much reminiscent of that in haloperoxidases, with the exception that histidine is replaced by cysteine.<sup>[11]</sup> Inhibition of a protein tyrosine–phosphatase by vanadate has been noted as a possible key step<sup>[12]</sup> in the insulin-mimetic action of inorganic and organic (coordination) compounds of vanadium.<sup>[13]</sup>

Vanadium complexes undergo a complex speciation pattern in extra- and intracellular body fluids, including hydrolysis, ligand exchange, and redox chemistry, the knowledge of which

[a] Prof. Dr. D. Rehder, Dr. D. Wang, Dipl.-Chem. A. Behrens, Dr. M. Farahbakhsh, Dipl.-Chem. J. Gätjens  
Institut für Anorganische und Angewandte Chemie  
Universität Hamburg, 20146 Hamburg (Germany)  
Fax: (+49) 40-4123-2893  
E-mail: dieter.rehder@chemie.uni-hamburg.de

is a precondition for understanding physiological effects of vanadium compounds. Several solution speciation studies modeling this situation with glutathione and related ligands have been carried out recently.<sup>[14, 15]</sup> The particularly important intracellular tripeptide glutathione GSH (where SH represents cysteine) and its oxidized form GSSG, which are present in millimolar concentrations and can redox-interact with vanadium,<sup>[16–18]</sup> have been shown to form a variety of complexes with VO<sup>2+</sup> in aqueous solution, including complexes with thiolate coordination to the vanadyl ion.<sup>[14, 15]</sup> The present study is designed to evidence the extent and quality of interactions between vanadium in various oxidation states and multifunctional ligands containing disulfide or thiolate functions, and thus modeling interactions of vanadium with peptides and proteins having cystine or cysteine constituents.

## Results and Discussion

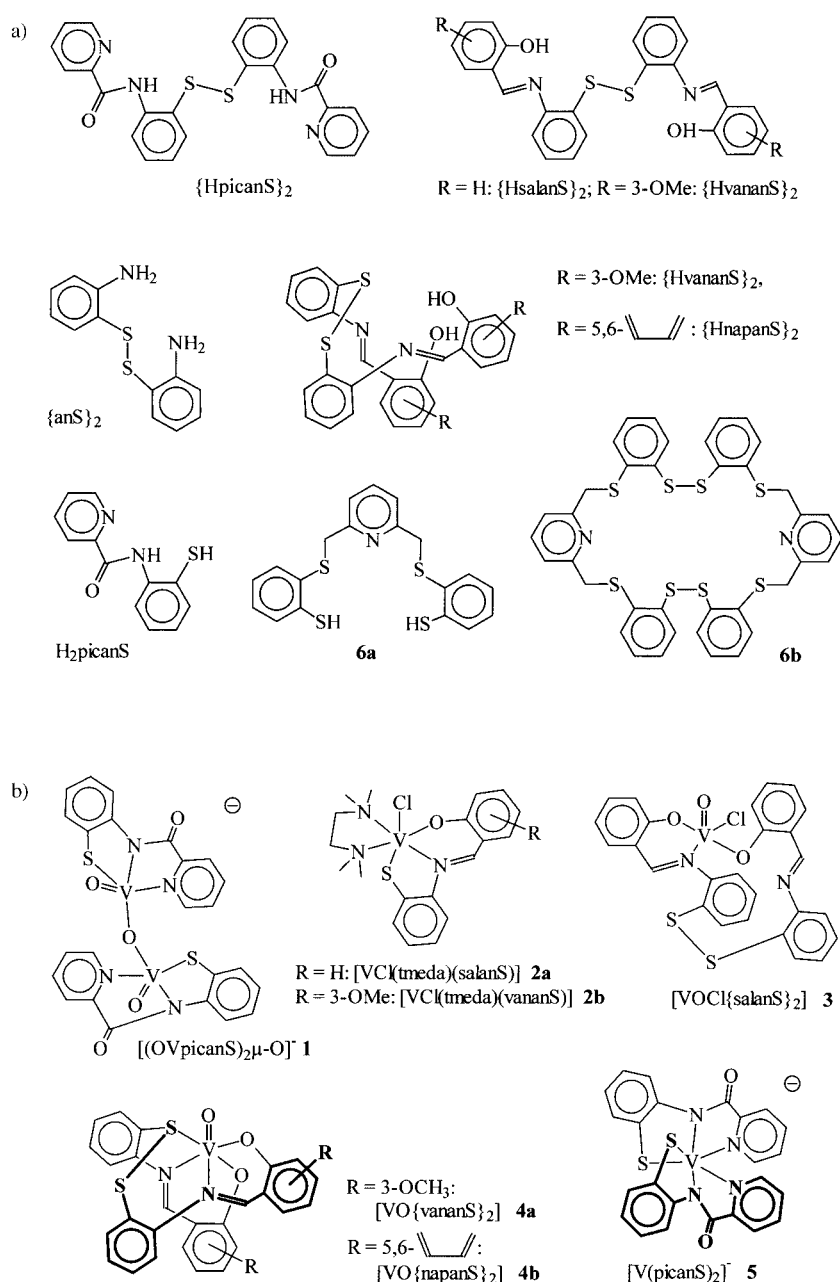
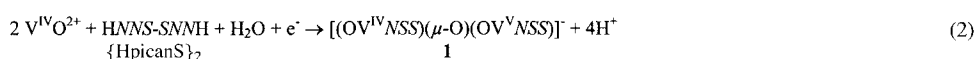
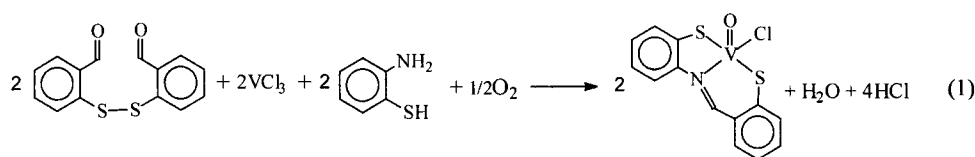
An overview comprising the ligands and complexes employed or characterized in this work is shown in Schemes 1a (ligands) and 1b (complexes).

### Cleavage of the disulfide bond:

We have previously shown<sup>[19]</sup> that the disulfide 2,2'-dithiodibenzaldehyde is reduced in a two-electron reduction by [VCl<sub>3</sub>(thf)<sub>3</sub>] to form, in the presence of 2-mercaptoaniline, a chlorooxovanadium(v) complex stabilized by the tridentate (SNS) Schiff base ligand originating from the condensation of mercaptoaniline and the product of the disulfide reduction, 2-mercaptobenzaldehyde

[Eq. (1)]. As shown in Equation (2) for the reaction between [VOCl<sub>2</sub>(thf)<sub>2</sub>] and the disulfide {HpicanS}<sub>2</sub>, {HNNS}<sub>2</sub> (letters in italics correspond to ligand functions), reductive cleavage of the sulfur–sulfur bond can also be initiated by (V<sup>IV</sup>O)<sup>2+</sup>. Anion **1** (see Sche-

me 1b) formed in this case is a dinuclear, oxo-bridged, mixed-valence anionic V<sup>IV</sup>V<sup>V</sup> complex containing the tridentate amide ligand picanS<sup>2-</sup> (NNS<sup>2-</sup>). The counterion in this reaction, which has been carried out in the presence of NEt<sub>3</sub> to capture the protons formed, is [HNEt<sub>3</sub>]<sup>+</sup>.



The additional oxygen atom presumably stems from residual water in the solvent THF; the second electron needed in this reaction may originate from a second vanadyl ion. The  $\nu(\text{CONH})$  associated with  $\{\text{HpicanS}\}_2$ ,  $1626\text{ cm}^{-1}$ , is shifted to  $1596\text{ cm}^{-1}$  in **1**, indicative of deprotonation of the amide in  $\text{picanS}^{2-}$ . Both nitrogen atoms, and the thiolate formed by reduction, coordinate to the vanadium center. There is a broad band for the  $\nu(\text{V}=\text{O})$  at  $991$  with a shoulder at  $981\text{ cm}^{-1}$ . The room-temperature EPR spectrum of **1** in THF shows two superimposed eight-line systems (coupling of the electron to the  $^{51}\text{V}$  nucleus (nuclear spin =  $7/2$ )) with significantly different  $g_0$  and  $A_0$  values, namely  $g_0 = 1.983$  and  $A_0 = 82 \times 10^{-4}\text{ cm}^{-1}$  for component 1, and  $g_0 = 1.97$  and  $A_0 = 101 \times 10^{-4}\text{ cm}^{-1}$  for component 2. The electron is thus not delocalized over the two vanadium sites; the two different vanadium sites, in which the single electron can reside, are about equally populated.

The inequivalence of the two oxo-linked building blocks of the dinuclear anion **1** is also revealed by the crystal structure determination of  $[\text{Et}_3\text{NH}]\text{-1} \cdot 0.5\text{NEt}_3$  (Figure 1). For selected

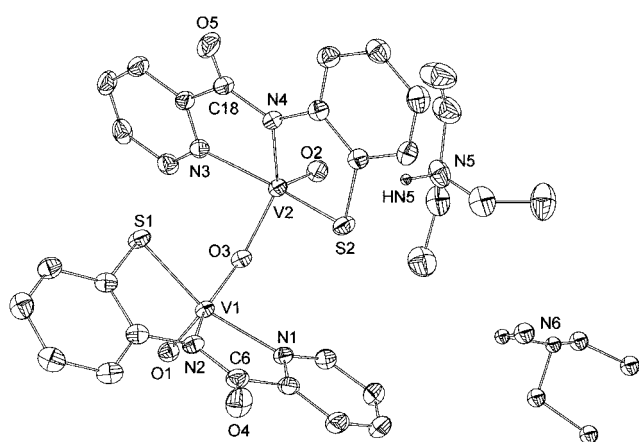


Figure 1. Structure of  $[\text{Et}_3\text{NH}][(\text{OVpicanS})_2\mu\text{-O}]$ ,  $[\text{Et}_3\text{NH}]\text{-1}$ , (ORTEP plot; 50% probability level) including one molecule of  $\text{NEt}_3$  of crystallization per 2 units of  $[\text{Et}_3\text{NH}]\text{-1}$ .

bonding parameters see Table 1. The counterion (N5) is linked to one of the doubly bonded oxo groups (O2) by an  $\text{N-H}\cdots\text{O}$  bond ( $2.856\text{ \AA}$ ). While one of the vanadium centers,

V1, is in an about ideal square-pyramidal array with the doubly bonded oxo group in the apical position and vanadium displaced from the plane N1N2S1O3 by  $0.0272\text{ \AA}$ , the other, V2, is in a somewhat distorted tetragonal-pyramidal environment, quantified by an angular  $\tau$  parameter of  $0.26$  ( $\tau = 0$  for an ideal square pyramid,  $\tau = 1$  for an ideal trigonal bipyramid). V2 is  $0.1161\text{ \AA}$  above the plane spanned by the three ligand functions and the bridging oxygen O3. O3 is not exactly in the center of the two vanadium ions;  $d(\text{V1-O3}) = 1.749(2)$ ,  $d(\text{V2-O3}) = 1.866(2)\text{ \AA}$ ; the angle V1-O-V2 amounts to  $135.06(10)^\circ$ . The V=O moieties are arranged in between the perpendicular and the *syn* configuration; the torsion angle O1,V1,V2/O2,V2,V1 is  $40.22^\circ$  and thus differs from the situation encountered in other mixed-valence dinuclear vanadium complexes such as *anti*- $\{[\text{VO}(\text{tacn})_2\mu\text{-O}]\}$  ( $176.5^\circ$ , tacn is a functionalized triazacyclononane),<sup>[20]</sup> *syn*- $\{[\text{VO}(\text{sal-ser})_2\mu\text{-O}]\}$  ( $11.6^\circ$ , sal-ser is the Schiff base from salicylaldehyde and serine),<sup>[21]</sup> or  $\{[\text{VO}(\text{sal-ala})_2\mu\text{-O}]\}$  ( $83.7^\circ$ ).<sup>[22]</sup> The  $d(\text{V-S})$  are comparable to those in most other thiolate complexes of  $\text{V}^{\text{IV}}$  and  $\text{V}^{\text{V}}$  (compare the discussion in reference [19]). Not unexpectedly, they are substantially shorter than in thioether complexes.<sup>[19, 23]</sup> The bonds to the pyridine-*N* atom are again in the usual range,<sup>[24]</sup> the bonds to the amide nitrogen atoms (N2 and N4),  $2.042(2)$  and  $2.031(2)\text{ \AA}$ , are slightly longer than reported in the literature (mean  $d(\text{V-N}_{\text{amide}}) = 2.014\text{ \AA}$ <sup>[25]</sup>).

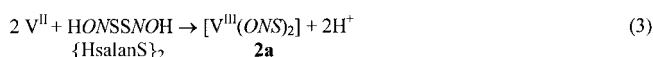
As can be expected for a  $\text{V}^{\text{II}}$  compound,  $[\text{VCl}_2(\text{tmeda})_2]$  (*tmeda* = *N,N,N',N'*-tetramethylethylenediamine) also reductively splits the disulfide bond in the double Schiff base disulfides derived from 2,2'-diaminodiphenyl disulfide and salicylaldehyde ( $\{\text{HsalanS}\}_2$ ) or 2-hydroxynaphthalene-1-carbaldehyde ( $\{\text{HvananS}\}_2$ ), *HONSSNOH*; see the idealized Equation 3. The structures of the disulfides are described below.  $\text{V}^{\text{II}}$  is oxidized to  $\text{V}^{\text{III}}$ , and the resulting Schiff base thiolates  $\text{salanS}^{2-}$  and  $\text{vananS}^{2-}$  substitute one *tmeda* and one chloro ligand to form the monochlorovanadium complexes **2a** and **2b**. The reaction is conducted in THF, yielding mixtures of **2** and the hydrochloride of *tmeda*; **2** can be isolated in analytically pure form by diffusion of pentane into the THF solution. The Raman spectrum of **2** no longer exhibits the band between  $500$  and  $550\text{ cm}^{-1}$  typical of the disulfide bridge.<sup>[26]</sup> The  $\nu(\text{HC}=\text{N})$  is shifted by  $10\text{ cm}^{-1}$  on coordination

Table 1. Selected bond lengths [ $\text{\AA}$ ] and angles [ $^\circ$ ] of vanadium complexes.

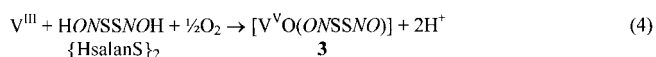
<b>1</b>				<b>3<sup>[a]</sup></b>		<b>5</b>	
V1–O1	1.6111(18)	V2–O2	1.612(2)	V–O2	1.589(3)	V–N1	2.1141(19)
V1–O3	1.7496(17)	V2–O3	1.866(2)	V–Cl	2.3690(14)	V–N3	2.1141(18)
V1–S1	2.3307(7)	V2–S2	2.3458(7)	V–O1	1.925(3)	V–N2	2.0582(18)
V1–N1	2.092(2)	V2–N3	2.097(2)	V–O3	1.986(3)	V–N4	2.0777(18)
V1–N2	2.042(2)	V2–N4	2.031(2)	V–N1	2.117(4)	V–S1	2.3481(7)
				N1–C15	1.304(6)	V–S2	2.3868(7)
V1–O3–V2	135.06(10)			N2–C12	1.308(6)		
O3–V1–O1	109.01(9)	O3–V2–O2	111.64(9)	S1–S2	2.0699(17)	N1–V–S1	159.91(6)
O3–V1–S1	92.84(6)	O3–V2–S2	92.92(6)			N3–V–S2	153.63(6)
O3–V1–N1	90.96(8)	O3–V2–N3	87.99(8)	Cl–V–N1	156.83(10)	N2–V–N4	173.52(7)
O3–V1–N2	146.47(8)	O3–V2–N4	136.81(8)	O1–V–O3	142.55(13)	S1–V–S2	103.47(3)
S1–V1–N1	145.45(6)	S2–V2–N3	152.52(6)	Cl–V–O2	103.71(13)	N2–V–N1	77.98(7)
N1–V1–N2	76.70(8)	N3–V2–N4	78.24(8)	Cl–V–O3	87.52(10)	N2–V–N3	97.03(7)
S1–V1–N2	81.40(6)	S2–V2–N4	82.47(6)	O1–V–N1	86.38(14)	N2–V–S1	83.17(5)
						N2–V–S2	152.52(6)

[a] Additional parameters for the disulfide moiety are provided in Table 3

(1613 and 1611 in **2a** and **2b**, 1603 and 1601  $\text{cm}^{-1}$  in free  $\{\text{HsalanS}\}_2$  and  $\{\text{HvananS}\}_2$ ).



**Preservation of the disulfide bond:** The mechanism of the rupture of the disulfide bond as catalyzed by metals may involve intermediate coordination of the electrophilic metal ion to (one of the sulfurs of) the disulfide.<sup>[27, 28]</sup> Disulfide complexes have been known since the work by Brändén,<sup>[29]</sup> although no such complex has so far been structurally characterized for vanadium. Our own efforts to prepare vanadium complexes of disulfides have lead to a structurally characterized complex with an intact, though uncoordinated, disulfide in the coordination sphere, **3**, and to disulfide complexes, structurally not characterized, where one of the sulfurs probably coordinates to vanadium, namely the complexes **4a** and **4b**, see Scheme 1b. The reactions leading to **3** and **4** are presented in idealized form in Equations (4) and (5).



Compound **3** is obtained from the reaction between  $[\text{VCl}_3(\text{thf})_3]$  and  $\{\text{HsalanS}\}_2$  in  $\text{CH}_2\text{Cl}_2$  in the presence of triethylamine as a proton scavenger. Oxygen present in the solution oxidizes  $\text{V}^{\text{III}}$  to oxovanadium(v), which coordinates to the dianionic ligand  $\{\text{salanS}^-\}_2$ ,  $^-\text{ONSSNO}^-$ . The characteristic  $\nu(\text{V}=\text{O})$  lies at  $992 \text{ cm}^{-1}$ . The  $\nu(\text{HC}=\text{N})$  of the free ligand,  $1613 \text{ cm}^{-1}$ , is split into two bands in **3**, shifted to  $1627$  and  $1607 \text{ cm}^{-1}$ , corresponding to uncoordinated and coordinated imine-*N* atoms in the complex. This situation is corroborated by the X-ray diffraction analysis of  $\mathbf{3} \cdot 3 \text{CH}_2\text{Cl}_2$  (Figure 2; selected bonding parameters are collated in Table 1). Although  $\{\text{salanS}^-\}_2$  usually functions as a pentadentate ligand,<sup>[30–33]</sup> only three of its functions are employed in coordination here, namely the two phenolate oxygen atoms O1 and O3, and one of the imine nitrogen atoms (N1), while

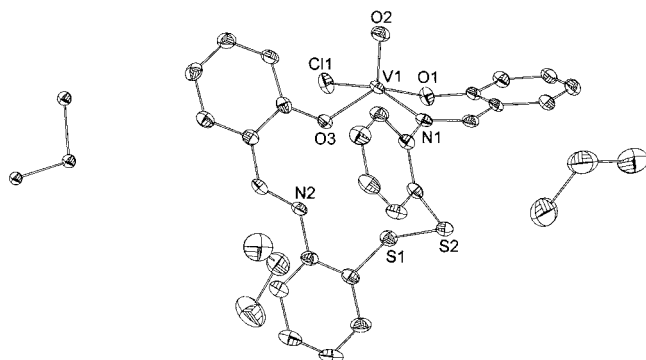


Figure 2. Structure of  $[\text{VOCl}\{\text{salanS}\}_2]$  (**3**) (ORTEP plot; 50% probability level), including the three  $\text{CH}_2\text{Cl}_2$  molecules of crystallization.

the two sulfur atoms S1 and S2 and the second imine group (N2) remain uncoordinated, the closest contact being that between V and S1 (4.29 Å), that is, clearly beyond the sum of the van der Waals radii. Despite this, the bond length  $d(\text{S1}–\text{S2}) = 2.070(2)$  is widened with respect to this distance in the free ligand  $\{\text{HsalanS}\}_2$  (2.026 Å; vide infra), but compares to  $d(\text{S1}–\text{S2})$  in metal complexes in which the sulfur binds to the metal.<sup>[30–33]</sup> The coordination sphere of **3** is supplemented by the doubly bonded oxo group and a chloro ligand. Vanadium, in a slightly distorted square-pyramidal environment ( $\tau = 0.28$ ), is displaced from the tetragonal plane formed by O1, O2, N1, and Cl by only 0.089 Å. All bond lengths involving vanadium are normal. The bonding parameters of  $\{\text{salanS}^-\}_2$  in complex **3** will be discussed in a broader context below.

Reaction of  $[\text{VO}(\text{van})_2]$  (Hvan = *o*-vanillin) or  $[\text{VO}(\text{nap})_2]$  (Hnap = 2-hydroxynaphthalene-1-carbaldehyde),  $[\text{VO}(\text{OO})_2]$  ( $\text{OO}^-$  is the aldehyde ligand) in Equation (5), with diamino-diphenyl disulfide ( $\{\text{anS}\}_2$ ) in dry THF yields the complexes **4a** and **4b** derived from the double Schiff-base ligands  $\{\text{HsalanS}\}_2$  and  $\{\text{HvananS}\}_2$  (see Scheme 1), which form by in situ condensation. The structure for **4** proposed in Scheme 1b is based on spectroscopic characteristics and elemental analyses. Thus, the IR bands (Table 2) characteristic of the aldehyde group of  $[\text{VO}(\text{OO})_2]$  and the amino groups of  $\{\text{anS}\}_2$  are no longer present in **4**. Instead, new IR absorptions appear for the newly formed  $\text{HC}=\text{N}$  moiety.

Table 2. Selected IR characteristics of the complexes **4** and their precursors.

	$\nu(\text{NH}_2)$	$\nu(\text{CHO})$	$\nu(\text{HC}=\text{N})$	$\nu(\text{V}=\text{O})$	$\nu(\text{V}–\text{S})$
$\text{VO}(\text{van})_2$		1657		958	
$\text{VO}(\text{nap})_2$		1686		978	
$\{\text{anS}\}_2$	3373, 3297				
<b>4a</b>			1603	985	362
<b>4b</b>			1617	982	358

The coordination of one of the sulfur atoms of the disulfide bond is supported by a  $\nu(\text{VS})$  around  $362 \text{ cm}^{-1}$  and the parallel (*z*) component of the EPR spectroscopic hyperfine coupling constant  $A_z = 162 \times 10^{-4} \text{ cm}^{-1}$ . Using the partial  $a_z$  values provided by Chasteen<sup>[34]</sup> and Kabanos et al.<sup>[35]</sup> for imine-*N* (44.1), phenolate-*O* (38.9), and thiophenolate-*S* (35.3) atoms, the calculated  $A_z$  originating from an  $\text{SNO}_2$  equatorial donor set amounts to  $156.9 \times 10^{-4} \text{ cm}^{-1}$ . We suppose, however, that a disulfide-*S* atom is a clearly weaker ligand than a thiolate-*S* atom and hence gives rise to a larger partial contribution than the latter, resulting in the observed value.

**Thiolato complexes, and the formation and characterization of disulfides:**  $\text{V}^{\text{III}}$  does not redox interact with thiolates; the anionic  $\text{V}^{\text{III}}$  thiolato complex **5** has thus been obtained by direct reaction of  $[\text{VCl}_3(\text{thf})_3]$  with the amide ligand  $\text{H}_2\text{picanS}$  (Scheme 1a) in dry THF plus  $\text{NEt}_3$ . Addition of triethylamine is necessary to promote deprotonation of the amide group and its coordination, along with the pyridine-*N* atom and the thiophenolate-*S* atom, to the vanadium center. A triethylam-

monium ion is the counterion for **5**. Complex **5** contains two nonequivalent picanS<sup>2-</sup> ligands, as evidenced by two amide bands in the IR spectrum (1611 and 1586; free H<sub>2</sub>picanS: 1690 cm<sup>-1</sup>), and by the molecular structure as revealed by X-ray structure analysis (Figure 3). The complex is distorted

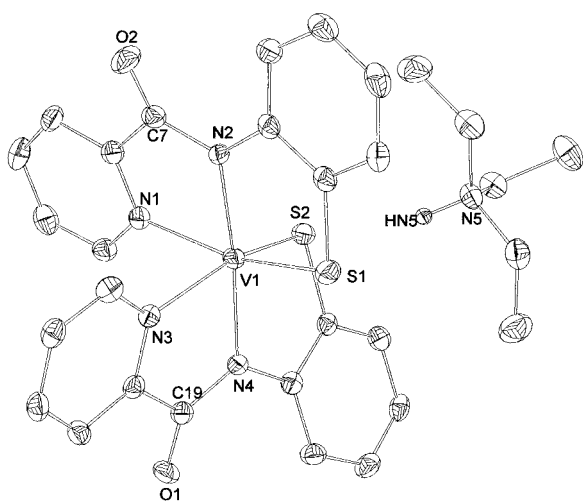
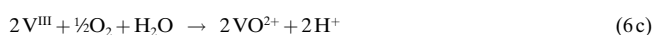
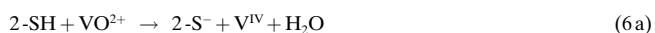


Figure 3. Structure of [Et<sub>3</sub>NH][V(picanS)<sub>2</sub>], [Et<sub>3</sub>NH]-**5** (ORTEP plot; 50% probability level).

octahedral. The two tridentate ligands occupy *meridional* positions, with the two amide-N atoms N2 and N4 *trans* to each other. Bonding parameters (Table 1) are in the usual range, except for the  $d(V-N_{\text{amide}})$  distances 2.058(2) and 2.078(2) Å, which are considerably longer than corresponding parameters reported in the literature (mean 2.014 Å<sup>[25]</sup>).

On the other hand, thiolates can be oxidized to disulfides in the presence of VO<sup>2+</sup>,<sup>[36–38]</sup> a reaction that can be accompanied by an abstraction of the oxo group<sup>[37, 38]</sup> and concomitant formation of non-oxo V<sup>IV</sup> complexes.<sup>[38]</sup> The VO<sup>2+</sup>-mediated oxidation of thiolate has also been observed for the reaction between the dithiolate **6a** and [VO(acac)<sub>2</sub>] (acac = acetylacetonate(1-)), which leads to the cyclic bis(disulfide) **6b** (see Scheme 1a). For the overall reaction we propose the sequence represented by Equation (6), in which the initiating step is the deoxygenation of the vanadyl group (Equation (6a)), followed by oxidation of thiolate to disulfide by V<sup>IV</sup> (Equation (6b)), and reconstitution of the vanadyl moiety by oxygen (Equation (6c)). The net reaction is therefore aerial oxidation of the thiolate, catalyzed by the vanadyl ion.



The *cyclo*-hexaeicosane **6b** (Figure 4) and the disulfide {HsalanS}<sub>2</sub> (Figure 5) were characterized by X-ray diffraction analysis. Selected structural data, including those for

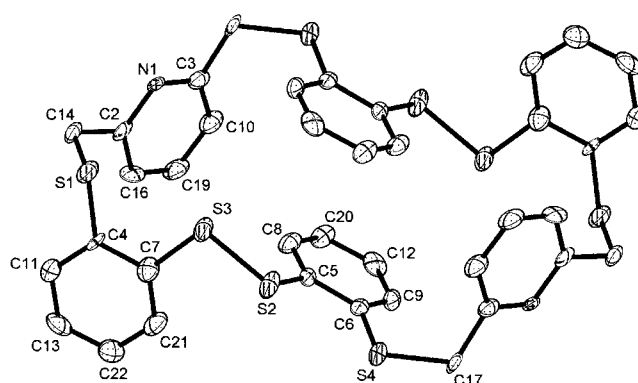


Figure 4. Structure of **6b** (ORTEP plot; 50% probability level).

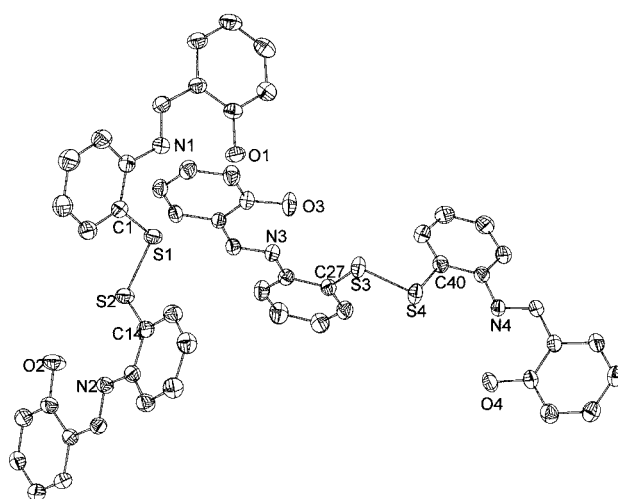


Figure 5. Structure of {HsalanS}<sub>2</sub> (ORTEP plot; 50% probability level). The two independent molecules in the unit cell are shown.

{salanS<sup>-</sup>}<sub>2</sub> of compound **3** are summarized in Table 3. The unit cell of {HsalanS}<sub>2</sub> contains two independent molecules in the “perpendicular” orientations to each other (Figure 5).

The two phenyl rings C5,C6,C9,C12,C20,C8 and (C5,C6,C9,C12,C20,C8)<sup>#</sup> in **6b** (point group C<sub>2</sub>) are parallel to each other; the distance between the two planes, 3.35 Å (the offset of the ring centers is 1.84 Å) suggests interaction. Bonding parameters are about equal for the three disulfides and, with the exception of  $d(\text{S-S})$ , also in the range noted for other disulfides.<sup>[39]</sup> The  $d(\text{S-S})$  in **6b** and {HsalanS}<sub>2</sub> are significantly shorter than in disulfides in general (av (2.072 ± 0.08) Å)<sup>[39]</sup> and, as far as **6b** is concerned, other cyclic bis(disulfides) such as tetrathia-*cyclo*-eicosanes in particular (2.083(1) Å).<sup>[36, 37]</sup> On the other hand,  $d(\text{S-S})$  of {salanS<sup>-</sup>}<sub>2</sub> in **3** falls within the range of average S-S distances in neutral disulfides, and in complexes where {salanS<sup>-</sup>}<sub>2</sub> coordinates in the pentadentate fashion, including coordination of one of the sulfurs.<sup>[30–33]</sup> Quite in contrast, the angles S-S-C in {salanS<sup>-</sup>}<sub>2</sub> in **3** are narrowed with respect to uncomplexed {HsalanS}<sub>2</sub> and other disulfides, where the  $\angle(\text{S-S-C})$  range from 102.6 to 104.8°, and this is also the case for the dihedral angle C1,S1,S2/C10,S2,S1, 72.14° in **3**, narrowed with respect to the corresponding angle in {HsalanS}<sub>2</sub> (82.34°) and other disulfides (av (82.1 ± 5.4)°). These differences apparently are due to the

Table 3. Bonding parameters of structurally characterized disulfides.

	$d(\text{S-S})$	$d(\text{S-C})$ S-S-C/C'-S-S	$\angle(\text{S-S-C})$	Dihedral angle
{HsalanS} <sub>2</sub>	2.026(2)	C1: 1.782(2), C14: 1.786(3)	C1: 104.64(9), C14: 105.40(11)	82.34
	2.027(2)	C27: 1.785(3), C40: 1.785(3)	C27: 105.36(11), C40: 105.30(10)	80.39
{salanS <sup>-</sup> } <sub>2</sub> in <b>3</b>	2.0699(17)	C1: 1.780(5), C10: 1.782(5)	C1: 100.30(16), C10: 98.95(16)	72.14
<b>6b</b>	2.039(3)	C5: 1.778(8), C7: 1.812(9)	C5: 104.7(3), C7: 104.4(3)	87.13

specific steric situation in **3**. Participation of the sulfur of {salanS<sup>-</sup>}<sub>2</sub> in coordination gives rise to further narrowing, see, for example, 55.4° in [NiCl{salanS}<sub>2</sub>] (55.4°).<sup>[33]</sup>

## Conclusion

With the present study we have provided evidence, including structural support, that vanadium, in its physiologically relevant oxidation state IV (and III<sup>[40, 41]</sup>) can form, break, and preserve the disulfide bond when interacting with organic disulfides and thiolates. The formation of disulfides via thiyl radicals has been shown to occur when thiolates such as cysteine are treated with vanadium(V) complexes.<sup>[42, 43]</sup> This reaction is of considerable relevance for the removal of V<sup>V</sup> in the intracellular medium (and hence for the detoxification of vanadate(V), an inhibitor of ATPases<sup>[44]</sup>), where glutathione (GSH) is a potent reducing agent,<sup>[16, 17, 45, 46]</sup> being itself oxidized to GSSG, although GSH can also be a slow and rather ineffectual reducing agent in vitro.<sup>[47]</sup> As shown by Equation (6), vanadyl ions (V<sup>IV</sup>O)<sup>2+</sup> are able to catalyze the aerial oxidation of thiolates. Under physiological conditions, a similar reaction can take place in the extracellular medium, and may also be anticipated for the cytoplasm in the presence of cytoplasmic oxygen, superoxide, or peroxide. GSSG makes up about 1–2% of the overall GSH + GSSG (2–3 mM) in erythrocytes;<sup>[48, 49]</sup> the reformation of GSH from GSSG, commonly achieved by the action of NADH, might also be mediated by VO<sup>2+</sup>; see Equation (1). Vanadyl ions can therefore attain a dual role in the GSH/GSSG transformation. In addition, VO<sup>2+</sup> can stabilize the disulfide bond ([Eq. (5)]) and thiolates by coordination. As was shown by solution speciation studies, this stabilization includes GSH, for which several vanadyl complexes have been proposed where cysteine participates in coordination.<sup>[15–17, 50]</sup> Another candidate for direct stabilization of thiolates is V<sup>III</sup>, which coordinates thiolates without concomitant redox events. Where VO<sup>3+</sup> is formed in redox interactions with disulfides, complex formation with the resulting thiolate ([Eqs. (1, 2)]) or the precursor disulfide ([Eq. (4)]) can occur. Transmitted again to the situation in biofluids, vanadium in its oxidation states V, IV, and III can be anticipated to be a subtle regulator of the GSH/GSSG equilibrium, and corresponding equilibria concerning other peptides with cysteine residues, by scavenging, redox-transforming and releasing thiolates and disulfides. To what extent cysteine and cystine moieties undergo redox interaction in the presence of vanadium also depends on the extent of their stabilization by complexation.

## Experimental Section

**Physical measurements:** Elemental analyses (C, H, N) were carried out on an Heraeus CHNO-Rapid analyser. IR spectra were recorded on a Perkin-Elmer 1720 spectrometer, using KBr pellets or nujol spreadings between KBr crystal plates. <sup>1</sup>H spectra were recorded on a Varian Gemini 200 MHz spectrometer with the usual parameter settings. EPR spectra were measured with a Bruker ESP 300E spectrometer at 9.74 GHz in 4 mm vials and concentrations of 1–5 mM at room temp. and at 97 K. Parameter adaptations were carried out with the program SimFonia (Bruker).

**X-ray structure analyses:** X-ray structure analyses were carried out in the  $\theta/2\theta$  scan mode either on an Enraf-Nonius CAD4 diffractometer with Cu<sub>K $\alpha$</sub>  irradiation (graphite monochromator,  $\lambda = 1.54178 \text{ \AA}$ ) at 173(2) K ([HsalanS]<sub>2</sub>), or on a Bruker SMART Apex CCD diffractometer with Mo<sub>K $\alpha$</sub>  irradiation (graphite monochromator,  $\lambda = 0.71073 \text{ \AA}$ ) at 153(2) K. For the solution and refinement of the structures, the program package ShelXTL 5.1 (Bruker 1998) was employed. Hydrogen atoms were placed into calculated positions and included in the last cycles of refinement. The protons directly attached to the nitrogen atoms of the [HNEt<sub>3</sub>]<sup>+</sup> counterions of **1** and **5** were located. Disorder of C62 (the CH<sub>3</sub> group of one of the ethyl substituents of the NEt<sub>3</sub> of crystallization in compound [Et<sub>3</sub>NH]**1**·0.5NEt<sub>3</sub>) was treated with a 60:40% model. Disorder of one of the CH<sub>2</sub>Cl<sub>2</sub> molecules in **3**·3CH<sub>2</sub>Cl<sub>2</sub> was treated in the following way: Cl6 versus Cl7 = 50:50%, Cl8 versus Cl9/Cl10 = 50:50%, and Cl9 versus Cl10 = 30:20%. The five C–Cl bond lengths in this model were fixed. Crystal and refinement data are collated in Tables 4 and 5. CCDC-192885 ([Et<sub>3</sub>NH]**5**), CCDC-192866 (**3**·3CH<sub>2</sub>Cl<sub>2</sub>), CCDC-192887 ([Et<sub>3</sub>NH]**1**·NEt<sub>3</sub>), CCDC-192888 ([HsalanS]<sub>2</sub>), and CCDC-192889 (**6b**) contain the supplementary crystallographic data for this paper. These data can be obtained free of charge via [www.ccdc.cam.ac.uk/conts/retrieving.html](http://www.ccdc.cam.ac.uk/conts/retrieving.html) (or from the Cambridge Crystallographic Centre, 12 Union Road, Cambridge CB2 1EZ, UK; Fax: (+44) 1223-336033; or deposit@ccdc.cam.ac.uk).

**Starting materials:** These were obtained from commercial sources or prepared according to literature procedures: [VOCl<sub>2</sub>(thf)<sub>2</sub>]<sup>[51]</sup> [VCl<sub>3</sub>(thf)<sub>3</sub>]<sup>[52]</sup> {HpicanS}<sub>2</sub> and H<sub>2</sub>picanS<sup>[53]</sup> **6a**·HCl<sup>[54]</sup> and [VCl<sub>2</sub>(tmeda)<sub>2</sub>]<sup>[55]</sup> The precursors [VO(aldehyde)<sub>2</sub>] were prepared and identified as described below, and used directly in the syntheses of **4a** and **4b**:

**[VO(*o*-vanillin)<sub>2</sub>]:** *o*-Vanillin (7.6 g, 0.05 mol), VOSO<sub>4</sub>·5H<sub>2</sub>O (6.32 g, 0.025 mol), and NaOAc·3H<sub>2</sub>O (6.8 g, 0.05 mol) were dissolved in deoxygenated water/ethanol 1.25:1 (80 mL). The solution was stirred for 2 h at room temperature. The green precipitate was collected by filtration, washed with ethanol and diethyl ether, and then dried in vacuo. Yield: 14.7 g (80%); IR (KBr):  $\tilde{\nu} = 3032$  (C–H<sub>arom</sub>), 978 (V=O), 737 cm<sup>-1</sup> (arom. aldehyde).

**[VO(2-hydroxynaphthalene-1-carbaldehyde)<sub>2</sub>]:** 2-hydroxynaphthalene-1-carbaldehyde (8.6 g, 0.05 mol), VOSO<sub>4</sub>·5H<sub>2</sub>O (6.32 g, 0.025 mol), and NaOAc·3H<sub>2</sub>O (6.8 g, 0.05 mol) were dissolved in deoxygenated water/ethanol 1.25:1 (80 mL). The solution was stirred for 4 h at room temperature. The green precipitate was collected by filtration, washed with ethanol and ether, and dried in vacuo. Yield: 14.3 g (70%); IR (KBr):  $\tilde{\nu} = 3050$  (C–H<sub>arom</sub>), 982 (V=O), 746 cm<sup>-1</sup> (arom. aldehyde).

### Preparation of the specific compounds

***N,N'*-(1,1'-dithiobis(phenylene))bis(salicylideneimine) ([HsalanS]<sub>2</sub>):** A solution of 2,2'-diaminodiphenyl disulfide (2.48 g, 10 mmol) in methanol (30 mL) was warmed to 40 °C and treated by stirring with salicylaldehyde

Table 4. Crystal data and structure refinement of complexes.

	[Et <sub>3</sub> NH]-1 · 0.5NEt <sub>3</sub>	3 · 3 CH <sub>2</sub> Cl <sub>2</sub>	[Et <sub>3</sub> NH]-5
empirical formula	C <sub>30</sub> H <sub>39.5</sub> N <sub>5.5</sub> O <sub>3</sub> S <sub>2</sub> V <sub>2</sub>	C <sub>29</sub> H <sub>24</sub> Cl <sub>7</sub> N <sub>2</sub> O <sub>3</sub> S <sub>2</sub> V	C <sub>30</sub> H <sub>32</sub> N <sub>5</sub> O <sub>2</sub> S <sub>2</sub> V
molecular mass [g mol <sup>-1</sup> ]	540.93	540.93	609.67
space group	<i>P</i> $\bar{1}$	<i>P</i> $\bar{1}$	<i>P</i> $\bar{1}$
<i>a</i> [Å]	8.7500(4)	11.9662(9)	10.6472(9)
<i>b</i> [Å]	10.8826(5)	13.2090(10)	10.9097(9)
<i>c</i> [Å]	18.4756(8)	13.7553(10)	12.8210(11)
$\alpha$ [°]	90.678(1)	65.150(1)	88.555(2)
$\beta$ [°]	102.990(1)	84.3596(1)	70.753(1)
$\gamma$ [°]	96.984(1)	65.950(1)	89.178(2)
volume [Å <sup>3</sup> ]	1700.16(13)	1473.9(2)	1405.5(2)
<i>Z</i>	2	2	2
$\rho_{\text{calcd}}$ [g cm <sup>-3</sup> ]	1.029	1.030	1.441
$\mu$ [mm <sup>-1</sup> ]	0.51	0.50	0.54
<i>F</i> (000)	536	522	636
crystal size [mm]	0.41 × 0.24 × 0.14	0.60 × 0.30 × 0.29	0.58 × 0.24 × 0.07
$\theta$ range [°]	1.13–25.00	1.69–25.00	2.17–27.50
limiting indices	–10 < <i>h</i> < 10 –12 < <i>k</i> < 12 –21 < <i>l</i> < 21	–11 < <i>h</i> < 14 –15 < <i>k</i> < 15 –16 < <i>l</i> < 14	–13 < <i>h</i> < 13 –7 < <i>k</i> < 13 –16 < <i>l</i> < 14
reflections collected	32 275	9640	9289
unique reflections	5982	6036	6022
<i>R</i> (int)	0.0377	0.0283	0.0212
refined parameters	433	395	368
Goof on <i>F</i> <sup>2</sup>	1.107	1.108	0.932
final <i>R</i> 1, <i>wR</i> 2 [ <i>I</i> > 2 $\sigma$ ( <i>I</i> <sub>0</sub> )]	0.0368, 0.1006	0.0709, 0.1715	0.0415, 0.0858
<i>R</i> 1, <i>wR</i> 2 (all data)	0.0423, 0.1114	0.0790, 0.1789	0.0586, 0.0909
diff. peak and whole [e Å <sup>-3</sup> ]	0.889, –0.295	1.106, –1.099	0.483, –0.411

Table 5. Crystal data and structure refinement of disulfides.

	{HsalanS} <sub>2</sub>	6b · 4THF
empirical formula	C <sub>26</sub> H <sub>20</sub> N <sub>2</sub> O <sub>2</sub> S <sub>2</sub>	C <sub>54</sub> H <sub>62</sub> N <sub>2</sub> O <sub>4</sub> S <sub>8</sub>
molecular mass [g mol <sup>-1</sup> ]	456.56	1059.54
space group	<i>P</i> $\bar{1}$	<i>P</i> 2 <sub>1</sub> / <i>c</i>
<i>a</i> [Å]	12.166(10)	8.6681(17)
<i>b</i> [Å]	12.380(12)	28.111(5)
<i>c</i> [Å]	16.84(2)	10.775(2)
$\alpha$ [°]	70.50(7)	
$\beta$ [°]	69.35(7)	93.485(4)
$\gamma$ [°]	89.84(7)	
volume [Å <sup>3</sup> ]	2219(4)	2620.7(9)
<i>Z</i>	4	2
$\rho_{\text{calcd}}$ [g cm <sup>-3</sup> ]	1.367	1.343
$\mu$ [mm <sup>-1</sup> ]	2.388	0.388
<i>F</i> (000)	952	1120
crystal size [mm]	0.45 × 0.40 × 0.30	0.82 × 0.30 × 0.14
$\theta$ range [°]	3.00–76.40	2.03–26.50
limiting indices	–15 < <i>h</i> < 5 –15 < <i>k</i> < 15 –21 < <i>l</i> < 19	–9 < <i>h</i> < 10 –34 < <i>k</i> < 34 –12 < <i>l</i> < 13
reflections collected	9845	16 166
unique reflections	9324	5389
<i>R</i> (int)	0.0094	0.0960
refined parameters	594	307
Goof on <i>F</i> <sup>2</sup>	1.069	1.182
final <i>R</i> 1, <i>wR</i> 2 [ <i>I</i> > 2 $\sigma$ ( <i>I</i> <sub>0</sub> )]	0.0443, 0.1203	0.1385, 0.3192
<i>R</i> 1, <i>wR</i> 2 (all data)	0.0463, 0.1226	0.1662, 0.3347
diff. peak and whole [e Å <sup>-3</sup> ]	0.367, –0.554	1.011, –0.794

(2.1 mL, 20 mmol). The yellow suspension thus obtained was refluxed for 2 h. This reaction mixture was cooled in an ice bath, whereupon a yellow solid precipitated, which was filtered off, washed with cold methanol

(60 mL), dried in vacuo and recrystallized from chloroform/DMF (1:1; 30 mL). Pure, yellow {HsalanS}<sub>2</sub> crystallized from this solution within two days in the form of small cubes suitable for an X-ray structural analysis. Yield 3.93 g (86 %); <sup>1</sup>H NMR ([D<sub>6</sub>]DMSO, TMS):  $\delta$  = 12.59 (s, 1H; Ph–OH), 9.04 (s, 1H; N=CH), 7.76–7.00 ppm (m, 8H; aromatic H); IR (KBr):  $\tilde{\nu}$  = 3459 (O–H), 3053 (C–H<sub>arom</sub>), 1613 (C=N), 1493 (C=C), 1464 (CH–S), 1280 (O–H), 1183 (CH–S wagging), 753 (*o*-subst. arom.), 713 (C–S), 463 cm<sup>-1</sup> (S–S); elemental analysis calcd (%) for C<sub>26</sub>H<sub>20</sub>N<sub>2</sub>O<sub>2</sub>S<sub>2</sub> (456.56): C 68.40, H 4.42, N 6.14; found: C 68.30, H 4.39, N 6.11.

***N,N'*-[1,1'-dithiobis(phenylene)]bis(3-methoxysalicylideneimine) ({HvananS}<sub>2</sub>):** This disulfide was prepared in an analogous fashion to {HsalanS}<sub>2</sub>, using *o*-vanillin (3.04 g, 20 mmol) dissolved in methanol (50 mL). Recrystallization from CHCl<sub>3</sub>/DMF (1:1; 40 mL) yielded orange needlelike crystals of {HvananS}<sub>2</sub> · 0.25 DMF. Yield 4.55 g (85 %); IR (KBr):  $\tilde{\nu}$  = 3050 (C–H<sub>arom</sub>), 2838 (C–H<sub>OMe</sub>), 1611 (C=N), 1566 (C=C), 1455 (CH–S), 1276 (O–H), 1250 (Ph–OMe), 1194 (CH–S wagging), 780 and 758 (*o*-subst. arom.), 734 (C–S), 455 cm<sup>-1</sup> (S–S); elemental analysis calcd (%) for C<sub>28</sub>H<sub>24</sub>N<sub>2</sub>O<sub>4</sub>S<sub>2</sub> · 0.25 DMF (534.90): C 64.55, H 4.85, N 5.89; found: C 64.50, H 4.25, N 5.62.

**[Et<sub>3</sub>NH][{VO(*N*-2-mercaptophenyl-2'-pyridinecarboxamide)}<sub>2</sub>O]**

**([Et<sub>3</sub>NH]-1):** [VOCl<sub>2</sub>(thf)<sub>2</sub>] (282 mg, 1 mmol), *N,N'*-[dithiobis(phenylene)-bis(pyridinecarboxamide)] ({HpicanS}<sub>2</sub>) (458 mg, 1 mmol) and NEt<sub>3</sub> (303 mg, 3 mmol) were dissolved in absolute THF (100 mL). The solution was refluxed overnight under N<sub>2</sub>, and then filtered. The precipitate was a mixture of complex [Et<sub>3</sub>NH]-1 and [NEt<sub>3</sub>H]Cl. IR (KBr):  $\tilde{\nu}$  = 1626, 1596 (C=O), 991 and 981 sh (V=O), 463 cm<sup>-1</sup> (V–S).

Dark green crystals of [HNEt<sub>3</sub>]-1 · 0.5NEt<sub>3</sub> with the same IR characteristics were obtained by redissolving the precipitate in CH<sub>2</sub>Cl<sub>2</sub>, and keeping the solution at –20 °C. The room-temperature EPR spectra of the crystals of [HNEt<sub>3</sub>]-1 dissolved in THF gave a two-component spectrum with the following parameters: *g*<sub>0</sub> = 1.983 and 1.97, *A*<sub>0</sub> = 82 and 101 × 10<sup>-4</sup> cm<sup>-1</sup>.

**[VCl{*N*-1-thiophenyl(salicylideneimine)}]tetramethylethylenediamine]**

**(2a):** A yellow solution of {HsalanS}<sub>2</sub> (457 mg, 1 mmol) in THF (20 mL) was warmed to 60 °C, and then treated dropwise, in an inert gas





- [36] W. Tsagkalidis, D. Rehder, *J. Biol. Inorg. Chem.* **1996**, *1*, 507–514.
- [37] W. Tsagkalidis, D. Rodewald, D. Rehder, *Inorg. Chem.* **1995**, *34*, 1943–1945.
- [38] M. Farahbakhsh, H. Nekola, H. Schmidt, D. Rehder, *Chem. Ber./Recueil* **1997**, *130*, 1129–1133.
- [39] M. Dötze, G. Klar, *J. Chem. Res. Synop.* **1993**, 226.
- [40] A. Stern, A. J. Davison, Q. Wu, J. Moon, *Arch. Biochem. Biophys.* **1992**, *629*, 95–106.
- [41] K. Kanamori, Y. Kinebuchi, H. Michibata, *Chem. Lett.* **1997**, 423–424.
- [42] X. Shi, X. Sun, N. S. Dalal, *FEBS Lett.* **1990**, *271*, 185–188.
- [43] E. G. Ferrer, P. A. M. Williams, E. J. Baran, *J. Trace Elements Med. Biol.* **1998**, *12*, 56–58.
- [44] P. J. Stankiewicz, A. S. Tracey, D. C. Crans in *Vanadium and Its Role in Life: Metal Ions in Biological Systems, Vol. 31* (Eds.: H. Sigel, A. Sigel), Marcel Dekker, New York, **1995**, ch. 9.
- [45] M. D. Cohen, A. C. Sen, C. Wei, *Inorg. Chim. Acta* **1987**, *138*, 91–93.
- [46] W. Legrum, *Toxicology* **1986**, *42*, 281–289.
- [47] J. Li, G. Elberg, D. Gefel, Y. Shechter, *Biochemistry* **1995**, *34*, 6218–6225.
- [48] H. K. Prins, J. A. Loos in *Biochemical Methods in Red Cell Genetics* (Ed.: J. J. Yunis), Academic Press, New York, **1996**, p. 115.
- [49] P. C. Jocelyn, *Biochem. J.* **1960**, *27*, 363–368.
- [50] A. Dessi, G. Micera, D. Sanna, *J. Inorg. Biochem.* **1993**, *52*, 275–286.
- [51] H. Tietz, K. Schmelik, G. Kreisel, *Z. Chem.* **1985**, *25*, 290–291.
- [52] L. E. Manzer, *Inorg. Synth.* **1982**, *21*, 138.
- [53] L. A. Tyler, J. C. Noveron, M. M. Olmstaed, P. K. Mascharak, *Inorg. Chem.* **2000**, *39*, 357–362.
- [54] D. Sellmann, J. Utz, F. W. Heinemann, *Inorg. Chem.* **1999**, *38*, 459–466.
- [55] J. J. H. Edema, W. Stauthamer, F. van Bolhuis, S. Gambarotta, W. J. J. Smeets, A. L. Spek, *Inorg. Chem.* **1990**, *29*, 1302–1306.

Received: September 17, 2002 [F4434]